Applied Catalysis B: Environmental 92 (2009) 1–8

Contents lists available at ScienceDirect

Applied Catalysis B: Environmental

journal homepage: www.elsevier.com/locate/apcatb

Review

Surface acid–basic properties of WOx–ZrO_2 and catalytic efficiency in oxidative desulfurization

G. Rodriguez-Gattorno [a], A. Galano [b,*], E. Torres-García [c,**]

[a] Centro de Investigaciones en Ciencias Aplicadas y Tecnologías Avanzadas del IPN, Legaria 694, Col. Irrigación, Del. Miguel Hidalgo, CP 11500, México DF, Mexico
[b] Departamento de Química, Universidad Autónoma Metropolitana-Iztapalapa, San Rafael Atlixco 186, Col. Vicentina, Iztapalapa, CP 09340, México DF, Mexico
[c] Instituto Mexicano del Petróleo, Eje Central Norte, Lázaro Cárdenas 152, San Bartolo Atepehuacan, 07730 México DF, Mexico

ARTICLE INFO

Article history:
Received 20 April 2009
Received in revised form 29 July 2009
Accepted 30 July 2009
Available online 8 August 2009

Keywords:
Tungstated zirconia
Brönsted and Lewis acidity
Surface acids
Dibenzothiophene
Oxidation

ABSTRACT

The dependence between catalytic activity of WOx–ZrO_2 system in the oxidation of dibenzothiophene (DBT) and its relationship with local acidity has been explored experimentally and theoretically. The structural requirements indicate that the oxidative efficiency (per W-atom) increases as the WOx surface density becomes larger, up to 7 W/nm^2. These results strongly suggest that n-meric domains and/or WO_{3-x} nanoparticles (NPs) anchored to surface are more reactive than monomeric and three-dimensional structures and that WOx domains of intermediate size provide the better compromise between surface acidity and catalytic efficiency. The experimental results suggest that catalytic efficiency is favored by the increasing of Brönsted acidity density. The theoretical analysis reveals that the combined presence of Lewis and Brönsted sites energetically favored the formation of peroxometallate complexes and that OOH addition reaches its maximum for minimum (non-zero) number of Lewis sites and maximum number of Brönsted sites.

Published by Elsevier B.V.

Contents

1. Introduction

It is well-known that the reactions of hydrogen peroxide with groups 5 and 6 metals in high oxidation states (e.g., Mo^{VI}, W^{VI}, V^{V}) produce peroxometallates complexes, which are efficient catalysts for oxidation reactions [1,2]. In particular, tungsten oxo-species supported on zirconia (ZrO_2) have been extensively studied and tested in different oxidation reactions with H_2O_2 [3,4]. These materials often show acidic properties and form an important class of solid acids [5,6]. However, only a small number of studies have been focused on establishing relationships between the acid–basic properties of the surface and its catalytic efficiency in heterogeneous reactions. The oxidative desulfurization (ODS) using tungsten peroxocompounds can be performed in homogeneous [2,7] and heterogeneous [3,8] conditions depending on the catalyst's nature. In both cases the tungsten compounds appear to be more a pre-catalyst than a catalyst and the experimental evidences suggest that activation consist in stabilization of peroxyl groups in the catalyst metal centers (W) which becomes the responsible specie for high efficiencies. For the case of heterogeneous catalyst, based on tungsten peroxo-species, most of the reports agree in the conclusion that there is a direct relationship

* Corresponding author.
** Corresponding author. Fax: +52 55 9175 8429.
E-mail addresses: agalano@prodigy.net.mx (A. Galano), etorresg@imp.mx, eneliot@yahoo.es (E. Torres-García).

0926-3373/$ – see front matter. Published by Elsevier B.V.
doi:10.1016/j.apcatb.2009.07.031

between acidity and efficiency in ODS processes [8–10]. Regardless of the numerous studies on the WO*x*–ZrO_2 system, the molecular and electronic structure of the active surface oxo-species is not yet fully understood. From previous works it is known, that the WO*x*–ZrO_2 system requires an exact control of surface acid properties, especially in reactions where the catalytic activity is justified by the presence of Brönsted acid sites [11–13]. In correspondence, three characteristics regions have been clearly identified: (i) low W densities ($\leq$5 W/nm^{-2}) where mainly monomeric oxo-species are present, (ii) intermediate W densities (within 5–8 W/nm^2 range) where, monomeric/polymeric oxo-species and crystalline WO_{3-x} nanoparticles (NPs) anchored to surface coexist, and (iii) high W densities ($\geq$9 W/nm^2) where crystalline WO_3 cluster aggregates are observed [11,13–16]. This suggests that at fixed rate W/Zr the real system consist in a broad equilibrium mixture of WO*x* species intermediates in the ZrO_2 surface. Investigations in this field are difficult and in most cases not very precise. This is in part due to the fact that it is often difficult to separate the influence of the different surface oxo-species. Hence, the need of building a predictive theoretical model for such complicated systems is critical. In a previous study, we have proposed different WO*x* molecular arrangements to mimic the local acid properties and we found that dimeric oxo-species are adequate to describe the acid–basic properties surface [13]. It is interesting to investigate the origin of the acidity in the WO*x*–ZrO_2 system and to establish its influence on the catalyst activity. For this propose, surfaces of WO*x*–ZrO_2 with different tungsten (W) loadings were tested in the oxidation reaction of dibenzothiophene (DBT). The results are used to propose a chemical approach to the relationship between surface acidity and catalytic efficiency in ODS of DBT. Theoretical Quantum calculations, in selected models with composition similar to most reactive species, allowed explaining the relationship among Brönsted and Lewis local acidity and the stabilization of possible responsible species for the oxidation of model compound (DBT).

2. Experimental

2.1. Catalyst preparation

High-surface-area $ZrO_{2-x}(OH)_{2x}$ (320 m^2/g) was prepared by precipitation from zirconium oxychloride solutions with ammonia as previously described [12]. The precipitate was filtrated and washed repeatedly by re-dispersion with a NH_4OH solution (pH 10) until the elimination of Cl^-, and then dried at 383 K for 24 h. Subsequently, $ZrO_{2-x}(OH)_{2x}$ was impregnated with an ammonium metatungstate solution, adjusted to pH 10 with ammonia, as reported in Ref. [11]. After drying at 383 K for 24 h, the samples were treated in flowing dry air for 3 h at 1073 K. The stabilized surface area of WO*x*–ZrO_2 in calcined samples was about 40–60 m^2/g. WO*x* surface densities were varied by changing the tungsten (W) concentration in order to obtain samples with WO*x* surface densities between 2 and 16 W/nm^2.

2.2. Catalytic test

A model solution was prepared with heptane (C_7H_{16}, 99.0 mol%) and DBT (98.0 mol%), with 0.0105 mol of total sulfur. The quantities of the reactants employed were 50 ml of model solution, 50 ml of acetonitrile (CH_3CN, 99.93 mol%), 0.2 ml of hydrogen peroxide (H_2O_2 at 30 wt.%) and 0.1 g of WO*x*–ZrO_2 catalyst. The reaction was carried out in a 250 ml glass batch Robinson–Mahoney reactor, equipped with a magnetic stirrer (1000 rpm) and a heated circulating bath. The temperature in the reactor was 60 °C. Samples at different time of reaction were taken and analyzed by a total sulfur analyzer (Horiba SFLA 1800) with an X-ray fluorescence detector and the accuracy of the reported values is estimated to be around 5%. The experimental details have already been reported [12].

2.3. Computational details

The calculations were performed with Gaussian 03 [17] package of programs. Geometry optimizations have been performed using the generalized gradient approximation (GGA), without any symmetry constraint. The Perdew and Wang's 1991 [18] functional (PW91) was used for exchange and correlation potentials. We have used the Dunning/Huzinaga valence double-zeta D95V [19] basis set for O, C, N and H atoms and the Stuttgart/Dresden [20] relativistic effective core potential (ECP) for W and Zr. Frequency calculations were carried out for all the studied systems at the same level of theory. Thermodynamic corrections at 298.15 K were included in the calculation of the relative energies. The stationary points were first modeled in gas phase (vacuum), and solvent effects were included *a posteriori* by single point calculations using polarizable continuum model, specifically the integral-equation-formalism (IEF–PCM) [21] at the same level of theory, with acetonitrile as solvent as in the experiments. For all modeled paths the solute cavity was computed using atomic radii from the universal force field (RADII = UFF), which assigns individual spheres to H atoms (explicit hydrogens).

3. Results and discussion

In order to establish the necessity of a rational design and an adequate balance between structure, local acidity, and electronic behavior of the active surface with the catalytic efficiency, WO*x*–ZrO_2 catalysts were tested in the ODS of DBT, using acetonitrile and hydrogen peroxide as extraction solvent and oxidant, respectively. Results of conversion as a function W/nm^2 and its relationship with surface acid site density (Brönsted and Lewis acid sites) for the sulfur oxidative compounds to a constant time (5 min) are shown in Fig. 1.

The tests show no catalytic activity at low surface density ($<$2 W/nm^2). Only at values above 2 W/nm^2 the catalysts begin to

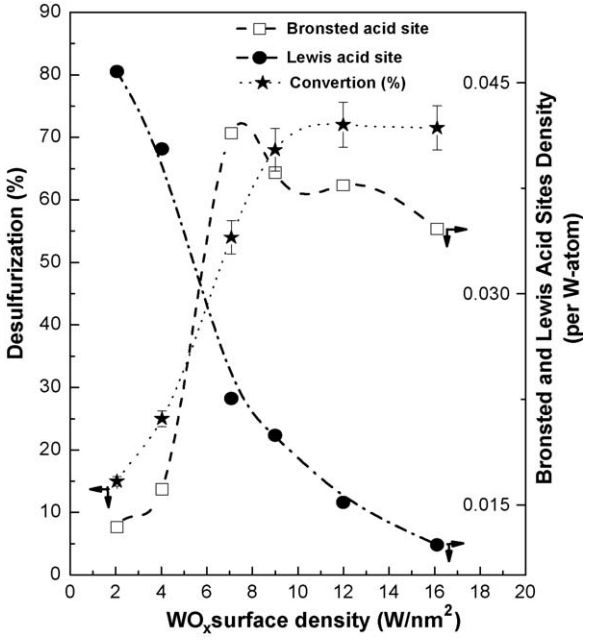

Fig. 1. Sulfur conversion as a function WO*x* surface density (W/nm^2) and its relationship with surface acid site density (Brönsted and Lewis acid sites, obtained by pyridine adsorption in situ using FT-IR (see details in Ref. [13]).

exhibit activity (~15% of conversion). By contrast, the conversion has a rapid evolution for W concentrations since 4–9 W/nm^2 presenting an important increase from ~25% up to ~70% conversion in that surface concentration range. In correspondence, experimental results from our group on the surface acid–base properties obtained by pyridine adsorption in situ using FT-IR spectroscopy [13], show that the surface density of Brönsted acid site (per W-atom) also increases exponentially with W loading between 4 and 7 W/nm^2, decreasing slightly for concentration above 7 W/nm^2. While, the density of Lewis sites (per W-atom) decreases in a markedly non-linear fashion in the same zone, up to 9 W/nm^2. It is interesting to notice that both, conversion and Brönsted acidity reach their maximum when Lewis acidity tends to a minimum. This suggests a direct relationship between catalytic activity and surface density of Brönsted acid sites (per W-atom).

We predict this behavior on the basis that the number of Brönsted sites increases while the Lewis acidity decreases as the W centers go from tetrahedral to octahedral coordination and as the condensation degree of the WO*x* domains increases. This strongly suggests that not all the Brönsted sites in the WO*x* domain are equally acid and that the changes in acidities for tungsten contents $\geq$7 W/nm^2 can be explained as a result of the increase in the degree of condensation towards a bulk-like behavior, which leads to an overall lowering in the specific surface acidity, in agreement with the results reported by Wachs et al. [16] and Iglesia et al. [22]. These considerations provide a viable explanation for the catalytic activity found in this work and for different catalytic process controlled by Brönsted acidity.

The catalytic efficiency expressed as transformed sulfur mol per minute normalized to site density (W/nm^2) at time of 5 min (initial rates) is shown in Fig. 2. The ODS efficiency, increases with increasing WO*x* surface density for surface densities up to 7 W/nm^2, suggesting that *n*-meric domains are more active than monomeric structures. Oxidative efficiency ultimately decreased at higher surface densities associated with the formation of three-dimensional species (presence of crystalline WO_3). Then, WO*x* domains of intermediate size apparently provide an adequate balance between sites nature, surface density of Brönsted and Lewis acid sites and catalytic efficiency during ODS of DBT.

This mechanistic conclusion would explain why the catalytic reaction reaches its maximum for a surface density between 6 and 8 W/nm^2 (see Fig. 2). These values can represent the point where the local coordination and polymerization degree of the WO*x* domains in mutual cooperation produce a maximum number of Brönsted sites per surface unit. However, up to this point our experimental results do not allow to establish the roll of both Brönsted and Lewis sites in the formation of a probable intermediate peroxometallate complex. Hence, the need of establish a predictive theoretical model.

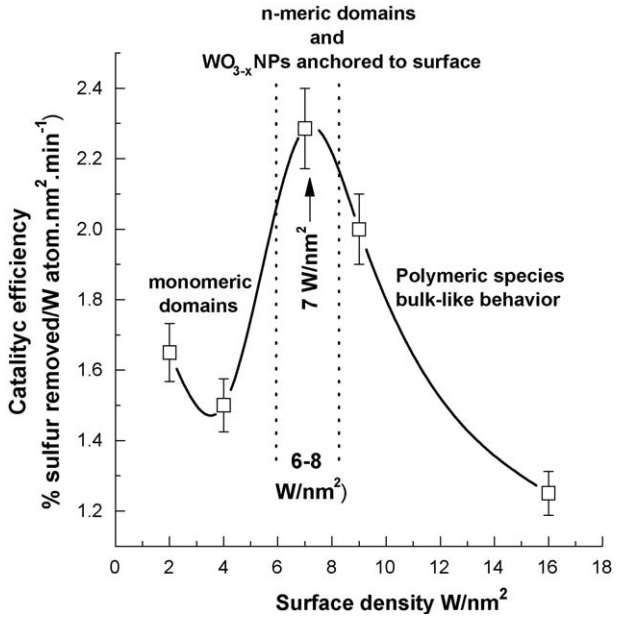

Fig. 2. Catalytic efficiency as a WO*x* function surface density W/nm^2.

4. Theoretical considerations

Although the catalytic oxidations of sulfur compounds with H_2O_2 in a polar solvent and different catalysts have been extensively studied in literature [8–10,23,24], the details on the compromise between site nature and reactivity in the reaction mechanism are still unclear. In this sense, two different hypotheses have been formulated to explain the formation of peroxotungstate sites, responsible for the catalytic activity of the WO*x*–ZrO_2 system. The first one assumes the interaction of H_2O_2 with W=O groups [25], while the second one involves the hydroxyl groups on the surface [26]. However, as our results show there is a direct relationship between the density of Brönsted acid sites and the catalytic efficiency of WO*x*–ZrO_2 system for sulfur conversion. Therefore, Brönsted sites are expected to play a role on the catalytic efficiency of WO*x*–ZrO_2, and probably on the peroxotungstates formation, that can only be justified by the hypothesis of Wong et al. [26].

To prove this hypothesis, the reactions of the hydroperoxyl radical with seven different WO*x*–ZrO_2 clusters have been computed. The hydroperoxide anion has not been considered since the deprotonation of H_2O_2 is expected to be negligible under the experimental conditions. This assumption is based on several facts. The actual peroxidation process is carried out at neutral pH in acetonitrile solutions. The pK_A value of hydrogen peroxide in aqueous solution is 10.67 [27]. This means that at neutral pH only the 0.002% of the total peroxide is in its deprotonated form (the distribution diagram is provided as Supporting Information: Fig. 1S). It is known that the degree of deprotonation of any acid in acetonitrile (ε = 36.64) solutions is lower than in water solutions (ε = 78.39). Therefore the fraction of peroxide that would be in its anionic form in acetonitrile is even lower than 0.002%, i.e., the concentration of hydroperoxide anion in the system is negligible. The radical (instead of anionic) peroxidation of this kind of system has been previously proposed by Santos et al. [28].

All models focus in the zone where catalytic reaction reaches its maximum: about ~5–7 W/nm^2. Seven different clusters have been chosen for mimicking materials having local configurations that resemble the expected species having an equivalent surface density about ~7 W/nm^2 (Fig. 3). The use of some simplified models to represent WO*x*–ZrO_2 systems has been validated in a previous work [13]. For the above mentioned composition we have tried different species varying the number of Brönsted and Lewis sites, in such a way that a wide variety of combinations have been modeled. By fixing the composition (W density) we intend to establish why and how the ODS process occurs for the system experimentally found as the most efficient.

Two steps of reaction have been modeled, namely the OOH addition to the catalyst (step I) and the water elimination (step II). In the particular case of cluster A the step II has been modeled as the OH elimination, since the starting cluster has no Brönsted sites and therefore water elimination is not possible. For clusters E and F two different paths of reaction have been computed, taken into account that the H_2O elimination can occur involving an OH moiety originally bonded to the same W-atom the OOH is adding to (a) or an OH moiety from the neighbor W-atom (b). In addition in cluster B, two different sites of reaction have been considered: one

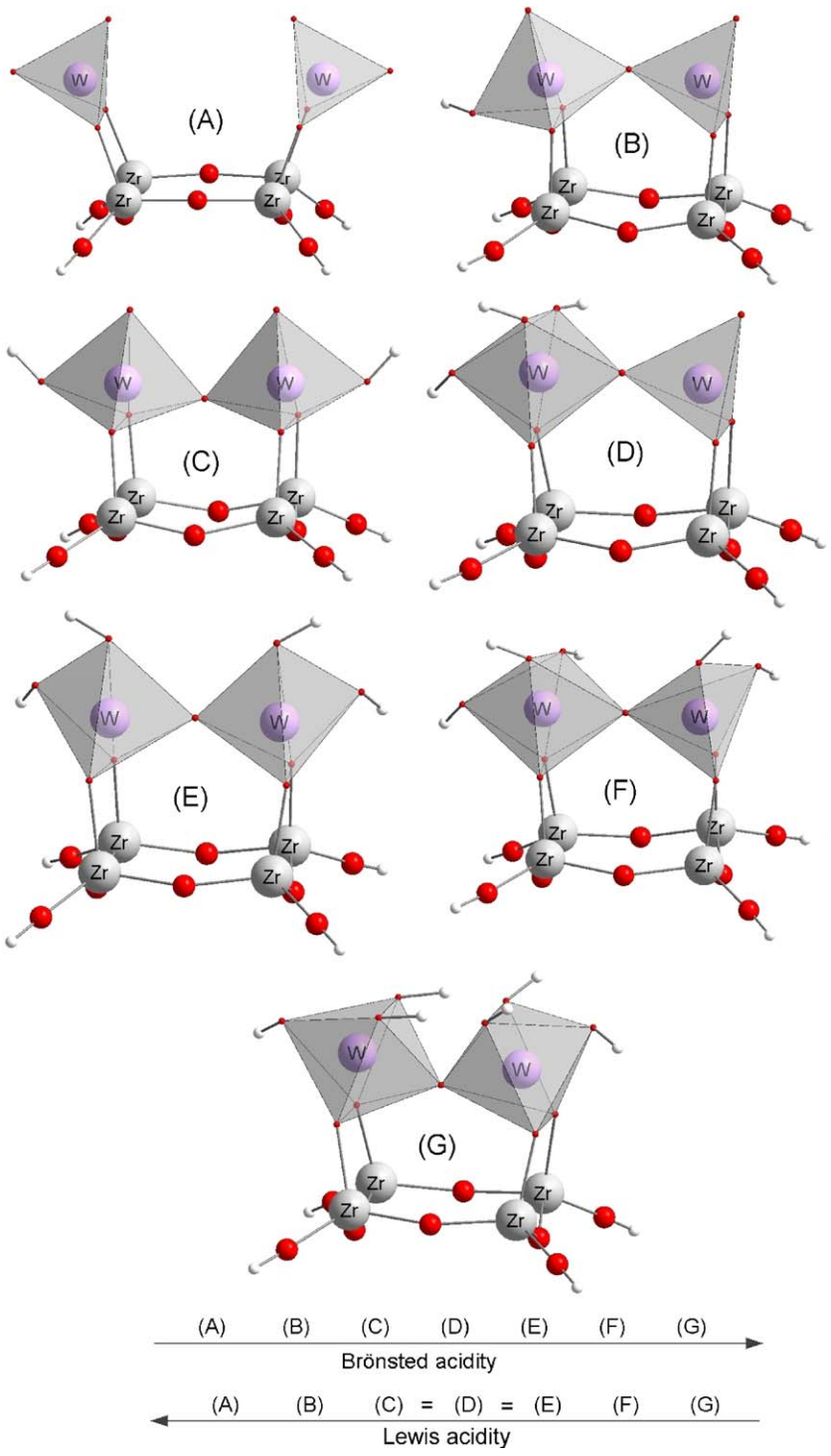

Fig. 3. Structure of the modeled clusters.

involving the W-atom with one Lewis site (B1) and the other involving the W-atom with two Lewis sites (B2).

All the OOH addition products, show intramolecular H bond interactions (Fig. 4). For the products formed from clusters B to G this interaction involves the H atom in the peroxyl radical, and one of the O atoms in the OH groups of the clusters. For cluster A, on the other hand, where there are no Brönsted sites in the starting reactant, the H atom in the peroxyl moiety migrates to one of the O atoms attached to the same W site the peroxyl group is attached to, and the intermolecular interaction occurs between this H and the O atom at the end of the peroxyl group.

The enthalpies and Gibbs free energies of reaction for the OOH addition processes are reported in Table 1. For gas phase, they were calculated using standard state of 1 atm, as calculated from the Gaussian program outputs. However, for reactions in solution the reference state has been changed from 1 atm to 1 M and the solvent cage effects have been included according to the corrections proposed by Okuno [29], taking into account the free volume theory [30]. These corrections are in good agreement with those independently obtained by Ardura et al. [31] and have been successfully used by other authors [32–35]. A detailed description of this approach can be found elsewhere [32–35].

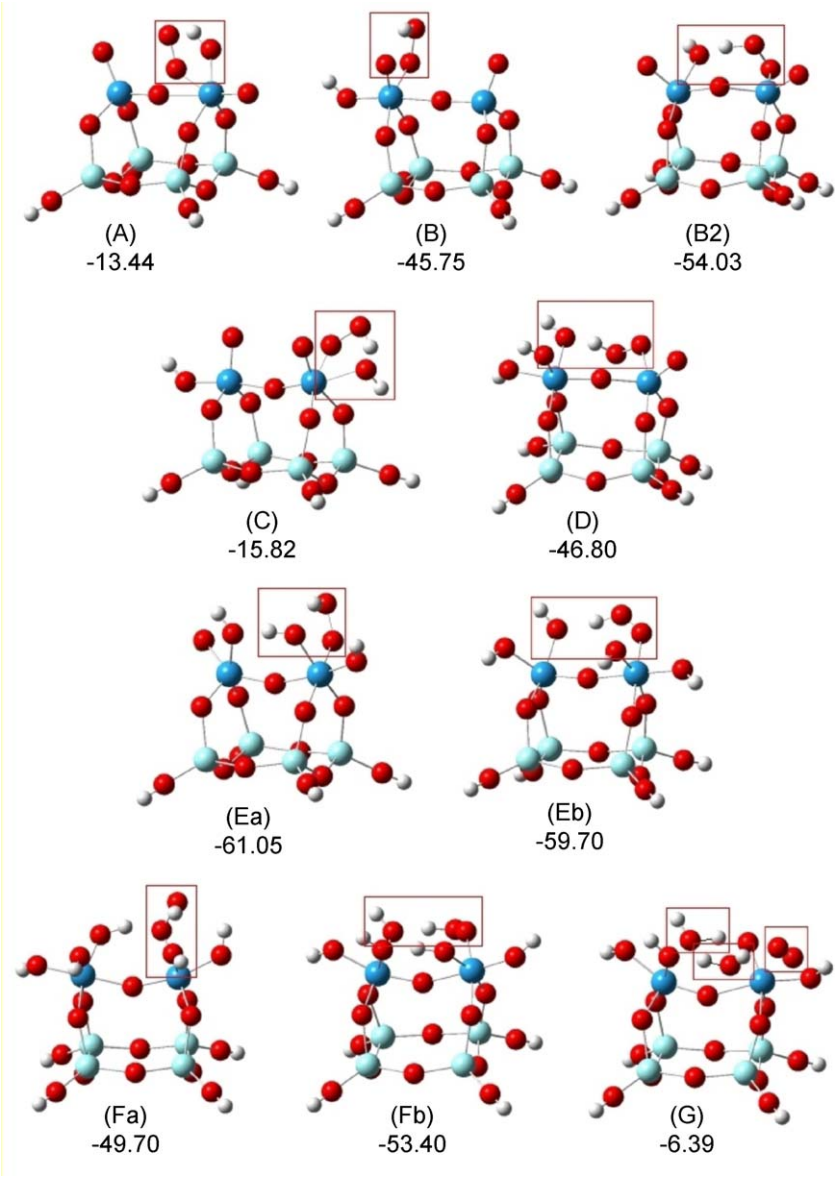

Fig. 4. Products of OOH addition (step I) and their Gibbs free energies in acetonitrile solutions (kcal/mol), relative to the starting reactants.

All the OOH addition processes were found to be exothermic and exergonic (Table 1). However, the addition most energetically favored is the one involving cluster E. This cluster has the largest number of Brönsted sites, with at least one Lewis site for one of the W-atoms. The least energetically favored additions are those involving clusters G and A, in that order, i.e., with minimum Lewis and Brönsted acidity, respectively (Fig. 6). These results suggest that the combined presence of Lewis and Brönsted sites facilitate the addition process. Apparently the viability of the OOH addition reaches its maximum when it takes place on a W-atom with only one Lewis site and with the maximum possible number of Brönsted sites, on this very W-atom and also on its next neighbors. When no Brönsted sites are present (A) the feasibility of the addition dramatically decreases, and if no Lewis sites are present (G) the reaction catalyst +OOH lead to a product that cannot be considered as a proper peroxometallate (Fig. 4). The resulting product rather corresponds to a complex where two water molecules were spontaneously expelled, and together with an O_2 molecule form a multi-fragment weak bonded complex with the remaining WO*x*–ZrO_2 structure. Clusters C, D and E have the same number of Lewis sites (2) but different numbers of Brönsted sites (2, 3, and 4, respectively). Therefore, comparing the ΔG values corresponding to OOH additions to these clusters would allow making assessments on the importance of the Brönsted acidity on the viability of the peroxidation processes. From values in Table 1 it can be easily noticed that as the number of Brönsted sites increase so does the exergonicity of the reaction.

Table 1
Enthalpies and Gibbs free energies of reaction (kcal/mol) for the addition reactions of OOH to the different modeled clusters.

	ΔH_{gas}	$\Delta H_{acetonitrile}$	ΔG_{gas}	$\Delta G_{acetonitrile}$
A	−33.44	−24.28	−18.37	−13.44
B1	−56.73	−54.48	−43.77	−45.75
B2	−70.95	−65.33	−55.42	−54.03
C	−26.36	−23.86	−14.09	−15.82
D	−66.40	−57.32	−51.65	−46.80
Ea	−72.47	−66.83	−61.10	−61.05
Eb	−72.22	−67.52	−61.52	−59.70
Fa	−67.02	−60.79	−51.70	−49.70
Fb	−72.07	−64.95	−56.28	−53.40
G	−22.17	−15.21	−9.12	−6.39

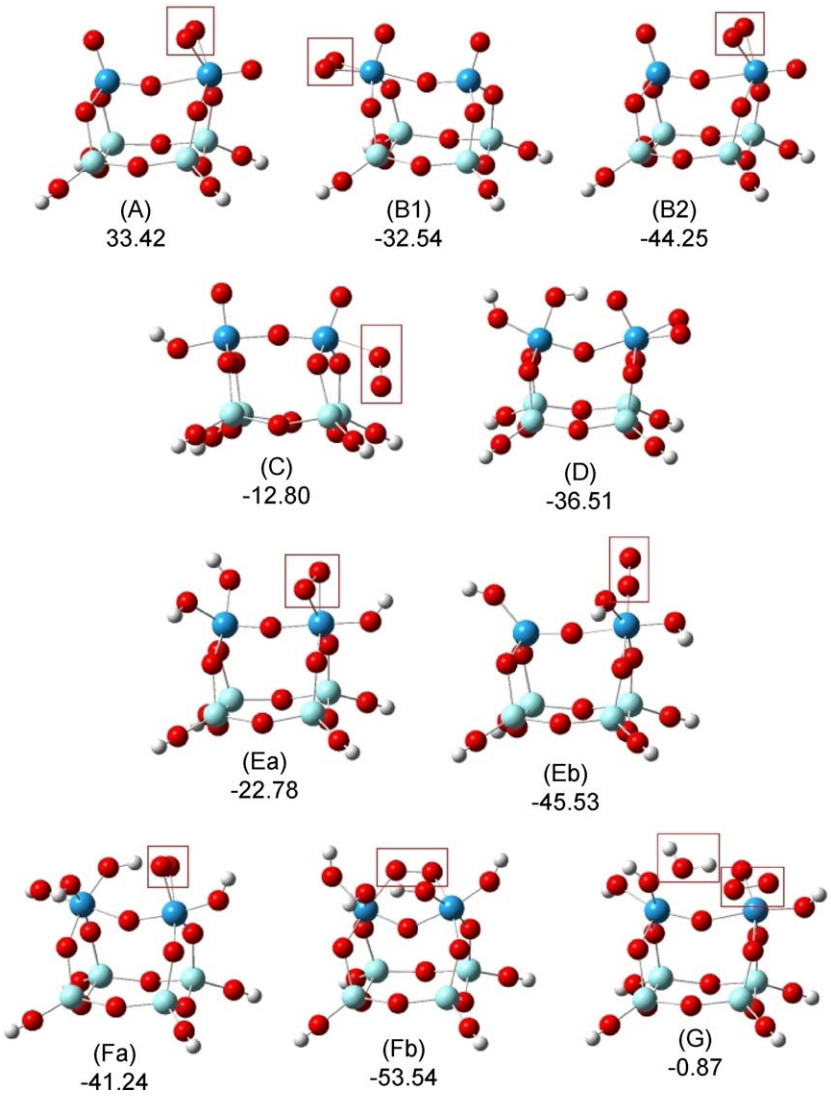

Fig. 5. Products of water elimination (OH elimination for cluster A, step II) and their Gibbs free energies in acetonitrile solutions (kcal/mol), relative to the starting reactants.

In addition, the water elimination processes from the addition products were also computed (Fig. 5) and even when the final products are lower in energy than the starting reactants (cluster +OOH) they are higher in energy than the addition products, with the exception of path Fb (Fig. 6). These results suggest that the condensation reactions would take place only in the vicinity of another chemical species promoting the dehydration. The reactivity of the different resulting peroxocomplexes is yet to be estimated.

In order to test the reliability of the calculated data, relevant geometrical parameters (W–O and O–O distances) of the modeled peroxotungstate species, before and after water elimination, have been compared to those reported in literature. They are reported in Table 2. As the values in this table show, the peroxidation products with geometrical parameters in agreement with the experimental results are those predicted as the most energetically favored. Products formed by OOH additions to clusters with no Lewis sites (G) or with no Brönsted sites (A) show the largest discrepancies. In fact for several reaction paths (B, D–F) the W–O and O–O distances of the modeled species have values that lie within the experi-

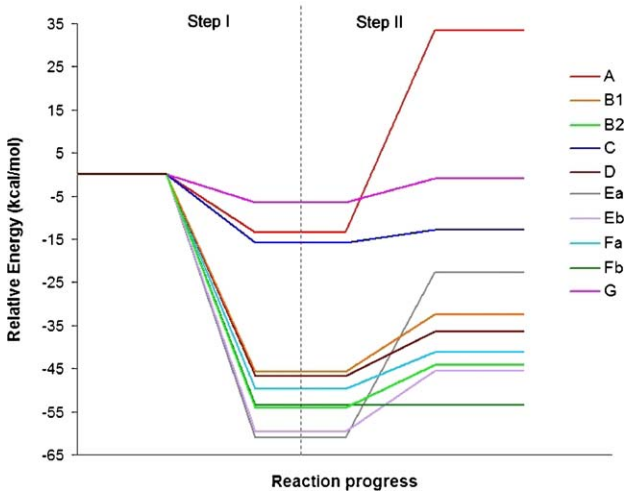

Fig. 6. Gibbs free energy evolution (kcal/mol). Step I: OOH addition and step II: H_2O elimination (OH elimination for cluster A).

Table 2
Selected geometrical parameters corresponding to hydroperoxide addition products (OOH), and to the products resulting from water loss (OO).

	d (W–O) (Å)	d (O–O) (Å)
A-OOH	2.19	1.38
B1-OOH	1.99	1.49
B2-OOH	2.01	1.53
C-OOH	2.21	1.38
D-OOH	1.98	1.52
E(a)-OOH	1.99	1.49
E(b)-OOH	1.91	1.48
F(a)-OOH	2.07	1.50
F(b)-OOH	1.94	1.46
G-OOH	2.34	1.37
A-OO	1.97	1.58
B1-OO	1.99	1.49
B2-OO	1.97	1.58
C-OO	2.28	1.38
D-OO	1.98	1.56
E(a)-OO	1.98	1.57
E(b)-OO	1.83	1.34
F(a)-OO	2.00	1.55
F(b)-OO	2.05	1.45
G-OO	2.20	1.38
Exp.	1.66–1.97 (Ref. [36]) 1.934–1.988 (Ref. [37]) 1.704–1.982 (Ref. [28])	1.53–1.63 (Ref. [36]) 1.499–1.504 (Ref. [37]) 1.486–1.5 (Ref. [28])

mental range, considering dispersion among the different sources. These results support the hypothesis that the observed peroxotungstate species are formed from WOx–ZrO_2 systems with relative large density of Brönsted sites, provided that they have at least one Lewis site. They also validate the methodology and models used in the presented calculations.

In addition, the calculated vibrational frequencies corresponding to the O–O stretching mode in peroxotungstate species have also been compared with the available experimental data (Table 3). However since the computed frequencies can have a systematic red (or blue) shifting with respect to the actual values, prior to trust them we are going to check the ν(O–O) value obtained with the same methodology for the free H_2O_2 molecule. The experimental value for this vibration is around 877 [38] to 879 cm^{-1} [40]. The non-scaled ν(O–O) calculated value is 863 cm^{-1}, i.e., about 15 cm^{-1} lower than the experimental data, which represents an excellent theory–experiment agreement. Accordingly, it seems reasonable to assume that computed the ν(O–O) calculated values for the modeled peroxotungstate species should lie in the vicinity of the accepted range ($\pm$15 cm^{-1}), defined from experiments. In Table 3 the structures that fulfill this criterion have been highlighted in black characters. As it was the case for geometrical parameters, only the calculated data for peroxotungstates formed from clusters A, C and G do not agree with the experimental values, within theoretical and experimental errors.

Table 3
Calculated vibrational frequencies for the O–O stretching mode in hydroperoxide addition products (OOH), and in the products resulting from water loss (OO).

X	ν(O–O) (cm^{-1})	
	X-OOH	X-OO
A	1061	823
B1	**871**	**867**
B2	**867**	823
C	1062	1070
D	**843**	**867**
E(a)	**881**	**850**
E(b)	**837**	1252
F(a)	**870**	817
F(b)	950	**897**
G	1068	1089
Exp.	843–883 (Ref. [36]) 843–845 (Ref. [39]) 860 (Ref. [40])	

Finally, from the combined analysis of experimental and theoretical results is possible to identify three main regions, associated with catalytic efficiency: (i) at very low loads of W ($\leq$4 W/nm^2) with scarce domains, essentially formed by isolated WO_4 or WO_6 monomers and lower catalytic activity, (ii) between 6 and 8 W/nm^2, with high catalytic efficiency, where n-meric domains of WOx and crystalline WO_{3-x} (NPs) anchored to the zirconia surface are expected to be the most abundant ones. Is just within this zone where, most probably the combined presence of Lewis and Brönsted sites facilitate the OOH addition process and (iii) at higher values ($\geq$9 W/nm^2), where presumably the octahedral polymeric species, besides the bulk-like WO_3 crystallites become the most abundant. In region (iii) the peroxometallate formation is not energetically favored. Any WOx load larger than that is expected to reduce the Brönsted acidity of the WOx–ZrO_2 system. Additionally, our theoretical results which correspond to the most probable clusters ($\sim$7 W/nm^2) support the observed strong dependence of catalytic efficiency with local Brönsted acidicity, which favored the formation of peroxotungstate. Following the TQC's the stabilization of peroxyl radical and the consequent formation of peroxometallate appears to be favored by mutual cooperation between local Lewis sites and Brönsted acid sites.

5. Conclusions

The experimental results indicate that oxidative efficiency (per W-atom) increases with increasing WOx surface density for surface densities up to 7 W/nm^2. This suggest that n-meric domain surfaces are more reactive than monomeric and three-dimensional structures and that WOx domains of intermediate size provide the most adequate balance between surface density of Brönsted and Lewis acid sites. The results suggest that the combined presence of Lewis and Brönsted sites in mutual cooperation energetically favors the OOH addition process and promotes the surface peroxometallate formation. Such that, the facility of the OOH addition reaches its maximum when it takes place on a W-atom with only one Lewis site and with the maximum possible number of Brönsted sites. It is the resultant of an adequate balance between local coordination, polymerization degree of the WOx domains and surface density of Brönsted acid sites.

Appendix A. Supplementary data

Supplementary data associated with this article can be found, in the online version, at doi:10.1016/j.apcatb.2009.07.031.

References

[1] W.R. Sanderson, Pure Appl. Chem. 72 (2000) 1289–1304.
[2] R.A. Sheldon, M. Wallau, I.W.C.E. Arendes, U. Schuchardt, Acc. Chem. Res. 31 (1998) 385–493.
[3] D.H. Koo, M. Kim, S. Chang, Org. Lett. 7 (2005) 5015–5018.
[4] F.M. Collins, R.A. Lucy, C. Sharp, J. Mol. Catal. A: Chem. 117 (1997) 397–403.
[5] T. Oufroy, G. Clet, M. Houalla, J. Phys. Chem. B 109 (2005) 3345–3354.
[6] V. Lebarbier, G. Clet, M. Houalla, J. Phys. Chem. B 110 (2006) 13905–13911.
[7] C.C. Dinoi, L. Gonsalvi, M. Peruzzini, E. Manoury, R. Poli., Organometallics 27 (10) (2008) 2281–2286.
[8] L.F. Ramírez-Verduzco, J.A. De los Reyes, E. Torres-García, Ind. Eng. Chem. Res. 47 (2008) 5353–5361.
[9] R.A. Sheldon, J.A. Van Doorn, J. Catal. 31 (1973) 427–437.
[10] F. Figueras, J. Palomeque, S. Loridant, C. Fèche, N. Essayem, G. Gelbard, J. Catal. 226 (2004) 25–31.
[11] A. Iribarren, G. Rodriguez-Gattorno, J.A. Ascencio, A. Medina, E. Torres-Garcia, Chem. Mater. 18 (2006) 5446–5452.

[12] E. Torres-Garcia, G. Canizal, S. Velumani, L.F. Ramirez-Verdusco, F. Murrieta-Guevara, J.A. Ascencio, Appl. Phys. A 79 (2004) 2037–2040.
[13] A. Galano, G. Rodriguez-Gattorno, E. Torres-Garcia, Phys. Chem. Chem. Phys. 10 (2008) 4181–4188.
[14] C. Angeles-Chavez, M.A. Cortes-Jacome, E. Torres-Garcia, J.A. Toledo-Antonio, J. Mater. Res. 21 (2006) 807–810.
[15] T. Kim, A. Burrows, C.J. Kiely, I.E. Wachs, J. Catal. 246 (2007) 370–381.
[16] E.I. Ross-Medgaarden, I.E. Wachs, J. Phys. Chem. C 111 (2007) 15089–15099.
[17] M.J. Frisch, G.W. Trucks, H.B. Schlegel, G.E. Scuseria, M.A. Robb, J.R. Cheeseman Jr., J.A. Montgomery, T. Vreven, K.N. Kudin, J.C. Burant, J.M. Millam, S.S. Iyengar, J. Tomasi, V. Barone, B. Mennucci, M. Cossi, G. Scalmani, N. Rega, G.A. Petersson, H. Nakatsuji, M. Hada, M. Ehara, K. Toyota, R. Fukuda, J. Hasegawa, M. Ishida, T. Nakajima, Y. Honda, O. Kitao, H. Nakai, M. Klene, X. Li, J.E. Knox, H.P. Hratchian, J.B. Cross, V. Bakken, C. Adamo, J. Jaramillo, R. Gomperts, R.E. Stratmann, O. Yazyev, A.J. Austin, R. Cammi, C. Pomelli, J.W. Ochterski, P.Y. Ayala, K. Morokuma, G.A. Voth, P. Salvador, J.J. Dannenberg, V.G. Zakrzewski, S. Dapprich, A.D. Daniels, M.C. Strain, O. Farkas, D.K. Malick, A.D. Rabuck, K. Raghavachari, J.B. Foresman, J.V. Ortiz, Q. Cui, A.G. Baboul, S. Clifford, J. Cioslowski, B.B. Stefanov, G. Liu, A. Liashenko, P. Piskorz, I. Komaromi, R.L. Martin, Dx.J. Fox, T. Keith, M.A. Al-Laham, C.Y. Peng, A. Nanayakkara, M. Challacombe, P.M.W. Gill, B. Johnson, W. Chen, M.W. Wong, C. Gonzalez, J.A. Pople, Gaussian 03, Revision E.01, Gaussian, Inc, Wallingford CT, 2004.
[18] J.P. Perdew, K. Burke, Y. Wang, Phys. Rev. B 54 (1996) 16533–16539 (and references therein).
[19] T.H. Dunning Jr., P.J. Hay, in: H.F. Schaefer, III (Ed.), Modern Theoretical Chemistry, vol. 3, Plenum, New York, 1976.
[20] (a) L.v. Szentpaly, P. Fuentealba, H. Preuss, H. Stoll, Chem. Phys. Lett. 93 (1982) 555–559;
(b) H. Stoll, P. Fuentealba, P. Schwerdtfeger, J. Flad, L.v. Szentpaly, H. Preuss, J. Chem. Phys. 81 (1984) 2732–2736;
(c) P. Fuentealba, H. Preuss, H. Stoll, L.v. Szentpaly, Chem. Phys. Lett. 89 (1989) 418–422.
[21] (a) M.T. Cances, B. Mennucci, J. Tomasi, J. Chem. Phys. 107 (1997) 3032–3041;
(b) B. Mennucci, J. Tomasi, J. Chem. Phys. 106 (1997) 5151–5158;
(c) B. Mennucci, E. Cances, J. Tomasi, J. Phys. Chem. B 101 (1997) 10506–10517;
(d) J. Tomasi, B. Mennucci, E. Cances, Theochemistry 464 (1999) 211–226.
[22] R.D. Wilson, D.G. Barton, C.D. Baertsch, E. Iglesia, J. Catal. 194 (2000) 175–187.
[23] V. Hulea, A.L. Maciuca, F. Fajula, E. Dimitriu, Appl. Catal. A: Gen. 313 (2006) 200–207.
[24] M. Te, C. Fairbridge, Z. Ring, Appl. Catal. A: Gen. 219 (2001) 267–280.
[25] (a) T. Pauporte, Y. Soldo-Olivier, R. Faure, J. Phys. Chem. B 107 (2003) 8861–8867;
(b) G.J. Colpas, B.J. Hamstra, J.W. Kampf, V.L. Pecoraro, J. Am. Chem. Soc. 118 (1996) 3469–3478.
[26] S.-T. Wong, C.-C. Hwang, C.-Y. Mou, Appl. Catal. B: Environ. 63 (2006) 1–8.
[27] G. Davies, N. Sutin, K.O. Watkins, J. Am. Chem. Soc. 92 (7) (1970) 1892–1897.
[28] I.C.M.S. Santos, F.A.A. Paz, M.M.Q. Simoes, M. Grac, P.M.S. Neves, J.A.S. Cavaleiro, J. Klinowski, A.M.V. Cavaleiro, Appl. Catal. A: Gen. 351 (2008) 166–173.
[29] Y. Okuno, Chem.-Eur. J. 3 (1997) 210–218.
[30] S.W. Benson, The Foundations of Chemical Kinetics, Krieger, FL, 1982.
[31] D. Ardura, R. Lopez, T.L. Sordo, J. Phys. Chem. B 109 (2005) 23618–23623.
[32] J.R. Alvarez-Idaboy, L. Reyes, J. Cruz, Org. Lett. 8 (2006) 1763–1765.
[33] A. Galano, J. Phys. Chem. A 111 (2007) 1677–1682 (Addition/Correction), 111 (2007) 4726–4726.
[34] J.R. Alvarez-Idaboy, L. Reyes, N. Mora-Diez, Org. Biomol. Chem. 5 (2007) 3682–3689.
[35] A. Galano, A. Cruz-Torres, Org. Biomol. Chem. 6 (2008) 732–738.
[36] L. Salles, C. Aubry, R. Thouvenot, F. Robert, C. Doremieux-Morin, G. Chottard, H. Ledon, Y. Jeannin, J.M. Bregeault, Inorg. Chem. 33 (5) (1994) 871–878.
[37] M. Grzywa, W. Nitek, W. Lasocha, J. Mol. Struct. 828 (2007) 111–115.
[38] C. Camy-Peyret, J.M. Flaud, J.W.C. Johns, M. Noel, J. Mol. Spectrosc. 55 (1992) 84–91.
[39] P. Hazarika, D. Kalita, S. Sarmah, R. Borah, N.S. Islam, Polyhedron 25 (2006) 3501–3508.
[40] M. Kantcheva, C. Koz, J. Mater. Sci. 42 (2007) 6074–6086.